



OPEN Coactivation patterns reveal the abnormality of dynamic state transitions between different psychiatric disorders

Lianjie Niu^{1,7}, Wenshi Li^{2,7}, Yongtao Bai^{3,7}, Keke Fang³, Shaoqiang Han⁴, Peng Liu⁵, Jinrong Qu^{2,6}✉ & Xianfu Sun¹✉

There is growing interest in utilizing dynamic methods to investigate psychiatric disorders, particularly the transient dynamic approaches. However, current research predominantly focuses on dynamic abnormalities within a single psychiatric disorder compared to healthy controls, without considering the shared and specific features across different psychiatric conditions. The dynamic abnormality across psychiatric disorders remains unclear. In this study, we employed Co-activation Pattern (CAP) method to investigate the transient configurations of brain activity across different psychiatric conditions, including schizophrenia (SZ, $n = 37$); bipolar I disorder (BD, $n = 40$); attention-deficit/hyperactivity disorder (ADHD, $n = 37$), and healthy controls (HC, $n = 110$). By conducting k-means clustering analysis, we identified 10 transient activation patterns. Our findings reveal that the specificity of psychiatric disorders is reflected in the transition probabilities between states, with distinct state transition patterns observed across different disorders. Notably, abnormal state transitions are concentrated in the core states (State 1 and State 2), highlighting the common dynamic abnormalities across psychiatric conditions. These core states involve the activation of the attention network and the sensorimotor network and show significant associations with the functional gradient. Furthermore, we found that abnormalities in state transitions are associated with cognitive behavior. Overall, this work provides a dynamic network perspective for understanding the shared and specific characteristic of psychiatric disorders.

Keywords Co-activation patterns, State transition, Schizophrenia, Bipolar I disorder, Attention-deficit/hyperactivity disorder

Psychiatric disorders, such as schizophrenia (SZ), bipolar disorder (BD), and attention-deficit/hyperactivity disorder (ADHD), have historically been conceptualized as independent diagnostic categories with distinct etiologies and clinical presentations. However, accumulating evidence suggests that the boundaries between different psychiatric disorders are not as clear-cut as traditionally believed. Recent researches have increasingly highlighted the overlapping symptoms, shared genetic factors, and common neurobiological pathways among various psychiatric conditions^{1–3}. For instance, Caspi et al. introduced the concept of the “p-factor,” which posits a general psychopathology factor that contributes to the risk of developing a wide range of psychiatric disorders⁴. Additionally, Kendler et al. found substantial genetic correlations between major psychiatric disorders, suggesting shared etiological pathways⁵. Such findings challenge the traditional view of psychiatric disorders as isolated entities and support the hypothesis that broad etiological and mechanistic overlaps exist across disorders.

¹Department of Breast Disease, Henan Breast Cancer Center, The Affiliated Cancer Hospital of Zhengzhou University, Henan Cancer Hospital, 127 Dongming Road, 450003 Jinshui, Zhengzhou, Henan, China. ²Radiology department, The Affiliated Cancer Hospital of Zhengzhou University and Henan Cancer Hospital, Zhengzhou 450003, Henan, China. ³Department of Pharmacy, The Affiliated Cancer Hospital of Zhengzhou University and Henan Cancer Hospital, Zhengzhou 450003, Henan, China. ⁴Department of Magnetic Resonance Imaging, the First Affiliated Hospital of Zhengzhou University, Zhengzhou 450052, Henan, China. ⁵Department of Otolaryngology, The Third Affiliated Hospital of Zhengzhou University, Zhengzhou 450052, Henan, China. ⁶Department of medical imaging department, The Affiliated Cancer Hospital of Zhengzhou University and Henan Cancer Hospital, 127 Dongming Road, 450003 Jinshui, Zhengzhou, Henan, China. ⁷Lianjie Niu, Wenshi Li and Yongtao Bai contributed equally to this work. ✉email: qjryq@126.com; zlyysunxianfu1256@zzu.edu.cn

Thus, transdiagnostic studies are crucial for identifying fundamental processes underlying multiple psychiatric disorders. By conducting transdiagnostic models, researchers can uncover shared and specific neurobiological abnormalities, enhancing our understanding and leading to more effective diagnostic and therapeutic strategies.

Resting-state functional magnetic resonance imaging (rs-fMRI) has been extensively utilized to capture the functional organization of brain, known as resting state functional connectivity (RSFC). Given that psychiatric disorders are characterized by the disruptions in large-scale brain network organization, RSFC provides a valuable tool for investigating brain network abnormalities across psychiatric disorders. Previous studies have revealed significant overlap in the neural circuits affected by different disorders, indicating shared neurobiological mechanisms^{6–8}. For example, disruptions in the default mode network (DMN) and Ventral attention network (VAN) are commonly observed in conditions such as schizophrenia, bipolar disorder, and major depressive disorder^{9,10}. These intrinsic functional networks are critical for cognitive and emotional processes, and their dysfunction may underlie the symptoms observed in these disorders. Notably, using latent components analysis, Kebets et al. identified distinct dimensions of functional connectivity patterns that span diagnostic categories, providing potential intermediate phenotypes linking psychiatric disorders¹¹.

Studies of static functional connectivity have significantly advanced our understanding of the disruption of functional networks in the brain across psychiatric disorders. However, the brain operates as a dynamic system, with its intrinsic dynamics underpinning complex cognitive flexibility, which is the ability to switch between different mental states to achieve various goals^{12,13}. Therefore, employing dynamic or time-varying approaches to explore dysfunction patterns in functional brain activity and large-scale functional connectivity networks may provide deeper insights into psychiatric psychopathology. By conducting dynamic functional connectivity, Li et al. indicated a common dysconnectivity which is dynamic state-dependent¹⁴. A promising approach for dynamic analysis is the Coactivation Pattern (CAP) analysis. CAP analysis is a data-driven method that clusters brain activity at time point to identify stable states, capturing the instantaneous dynamics of brain networks^{15–19}. Unlike the sliding-window approach, which requires predefined window sizes and shapes, CAP analysis does not rely on such presets, making it more flexible and sensitive to transient brain states. CAP analysis has been extensively applied to explore dynamic abnormalities in various diseases, offering valuable insights into their neural underpinnings²⁰.

In this study, we used a publicly available dataset from University of California, Los Angeles Consortium for Neuropsychiatric Phenomics (UCLA CNP), which includes neuroimaging and behavioral assessment across SZ, BD, and ADHD. Using CAP analysis, we characterized the dynamic transient configurations of brain activity across these psychiatric conditions. Our primary aim was to explore the abnormality of brain dynamics across multiple psychiatric disorders, with a focus on identifying shared and specific patterns of brain state transitions.

Materials and methods

Participants

In our study, we used data from University of California, Los Angeles Consortium for Neuropsychiatric Phenomics (UCLA CNP), which is available in the public database OpenfMRI²¹. This data consists of multimodal neuroimaging and behavioral data from 272 subjects, which include schizophrenia (SZ), bipolar disorder (BD), and attention-deficit/hyperactivity disorder (ADHD). Participants in the healthy control (HC) group had no lifetime diagnoses of psychotic or mental disorders, nor any history of substance abuse. For the patient group, all participants were diagnosed according to Structured Clinic Interview for DSM-IV-Text Revision. Each patient group (SZ, BD, and ADHD) excluded participants with any of the other diagnoses, ensuring that participants had only a single diagnosis. Participants provided written informed consent after receiving a verbal explanation of the study, following protocols approved by the Institutional Review Boards at UCLA and the Los Angeles County Department of Mental Health. All procedures were conducted in accordance with the ethical standards outlined in the Declaration of Helsinki. More detailed information about UCLA CNP dataset are included in previous study²¹. In our study, the participants who missing the MRI scans, behavioral scores, or had signal dropout in the cerebellum was excluded. Finally, a total 224 participants which included 37 patients with SZ, 40 patients with BD, 37 patients with ADHD, and 110 HCs were utilized for following analysis. The demographic data of selected participants were summarized in Table 1. For a comprehensive understanding of the clinical and behavioral assessments of this publicly available dataset, please refer to the detailed description provided in previous study²¹.

Data acquisition and preprocessing

Structural and functional MRI data were acquired on two 3T Siemens Trio scanners at UCLA. High-resolution anatomical data were collected by Magnetization Prepared Rapid Acquisition Gradient Echo (MPRAGE) scans using following parameters: TR = 1.9 s, TE = 2.26 ms, FOV = 250 mm, matrix = 256 × 256, sagittal plane, slice thickness = 1 mm, 176 slices. Functional data were collected using a T2*-weighted echoplanar imaging sequence (EPI) acquired using following parameters: slice thickness = 4 mm, 34 slices, TR = 2 s, TE = 30 ms, flip angle = 90°, matrix 64 × 64, FOV = 192 mm, oblique slice orientation. For each subject, the functional scanning contained 142 time points, representing 142 snapshots of whole-brain activity.

Resting state fMRI were preprocessed by fMRIPrep pipeline²² and connectome workbench tool²³. fMRIPrep is a robust and efficient tool designed for preprocessing fMRI data, providing standardized and automated workflows for generating high-quality, reproducible analysis results²². It leverages various open-source tools (such as ANTs, FSL, FreeSurfer) to perform a wide range of preprocessing steps. The following steps were applied to all participants based on fMRIPrep: skull stripping, motion correction, slice time correction, susceptibility distortion correction, and co-registration of the functional and anatomical scans. Motion artifacts were automatically removed from the pre-processed BOLD time-series using independent component analysis (ICA-

	HC	SZ	BD	ADHD	P value
Participants, n	110	37	40	37	
Age	31.3±8.7	35.5±9.0	34.8±9.2	31.2±10.1	0.03 ^a
Sex, male/female	57/53	29/8	23/17	20/17	0.041 ^b
Lifetime SUB ^c , n	41	26	34	22	
Adult Self Report Scale (ADHD symptoms)	8.6±2.7	9.4±4.3	12.1±4.9	15.3±3.8	<0.001 ^a
Hopkins Symptom Checklist					
Depression	0.37±0.35	0.79±0.60	0.91±0.63	0.66±0.46	<0.001 ^a
Obsessive compulsiveness	0.50±0.43	1.01±0.60	1.1±0.77	1.2±0.70	<0.001 ^a
Anxiety	0.21±0.28	0.75±0.64	0.73±0.65	0.46±0.40	<0.001 ^a
Wechsler Adult Intelligence Scale					
Vocabulary	43.7±8.2	31.7±9.4	42.9±10.3	43.5±9.6	<0.001 ^a
Matrix reasoning	20.6±4.1	15.4±4.9	19.6±4.4	20.7±3.9	<0.001 ^a
Wechsler Memory Scale (Visual reproduction delayed recall)	32.8±8.5	23.8±10.8	26.8±10.2	29.9±9.3	<0.001 ^a

Table 1. Clinical and demographic data for patients and healthy controls. a: one-way ANOVA; b: Chi-square test; c: Lifetime substance use included substance abuse and/or dependence for nicotine, alcohol, cannabis, cocaine, amphetamine, sedatives/hypnotics/anxiolytics, inhalants, opioids, and hallucinogens.

AROMA). ICA-AROMA motion components were collected and used as noise regressors along with the mean physiological signals from White matter, CSF. Finally, the time series were band-pass filtered between 0.01 Hz and 0.1 Hz to eliminate low-frequency drifts (e.g., scanner drift, physiological noise)²⁴, and high-frequency noise (e.g., rapid head motion)²⁵. Spatial smoothing was then applied using a 6 mm² Gaussian kernel to compensate for inaccuracies in spatial registration, and enhance the signal-to-noise ratio by averaging neighboring voxels²⁶. Both band-pass filtering and spatial smoothing were performed using the connectome workbench tool.

Co-activation pattern analysis

Co-activation pattern analysis (CAP) is a dynamic functional analysis method which capture the stable and recurring states of functional brain activity of whole brain. The schematic diagram illustrating of CAP analysis is shown in Fig. 1(A, B, C). The analysis steps were as follow: For each subject, the functional activity (BOLD signal) of each brain region was extracted by Schaefer 7-network template²⁷. This template contains 100 brain regions mapped onto 7 intrinsic functional networks (ICNs) including the Visual network (VN), Somatomotor network (SMN), Dorsal attention network (DAN), Ventral attention network (VAN), Limbic network (LIM), Frontoparietal network (FPN), and Default network (DMN). The functional activity of each brain region was normalized by using z-score transformation, and a two-dimensional normalized activity matrix $X_i \in R^{142 \times 100}$ (the number of time points = 142, the number of brain regions = 100) for each subject was obtained. Next, we performed k-means clustering to identify co-activation patterns across all subjects. The number of clustering is the free parameter of clustering analysis, and its optimal value was determined using the following steps: (1) All participants were randomly divided into two equally sized “folds,” with each fold containing its respective normalized brain activity matrix. In machine learning, splitting data into multiple groups or “folds” is a common cross-validation technique. This approach ensures that clustering results are robust and not overly influenced by any specific subset of data. (2) For each fold, we performed k-means clustering analyses with k ranging from 2 to 20. The purpose of this step was to assess the stability of clustering centers across the two folds under varying values of k. (3) The clustering centers should be stable across different subjects. Thus, we calculated the Pearson correlation of clustering centers between two folds for each k. The value of k which yielded the most stable cluster centers—indicating high correlation between folds—was selected as the optimal parameter. After determining the optimal number of clusters (k), we performed k-means clustering on the entire dataset to obtain stable cluster centers, which were then identified as the co-activation patterns.

Dynamic properties of CAP states

To evaluate the dynamic properties within and between CAP states, we calculated two dynamic measures at the individual level. (1) Fractional occupancy: fractional occupancy is defined as the proportion of time visiting each state over the whole duration. (2) Transition probability matrix: each element A_{ij} represents the transition probability of CAP states from state i to state j , where i and j are different state indices.

To investigate the abnormality of dynamic properties across the different psychiatric disorders, we conducted the one-way ANOVA analysis to dynamic metric including the fractional occupancy and transition probability matrix. Then the post-hoc analysis was conducted by two-sample t-test between each pair of groups including HC, SZ, BD, ADHD, to identify the difference between these disorders.

Results

Co-activation patterns and brain states

By applying CAP analysis to functional brain activity, 10 stable co-activation patterns were identified under the optimal cluster number. As showed in Fig. 2, we analyzed the spatial topology of CAPs by assigning each brain

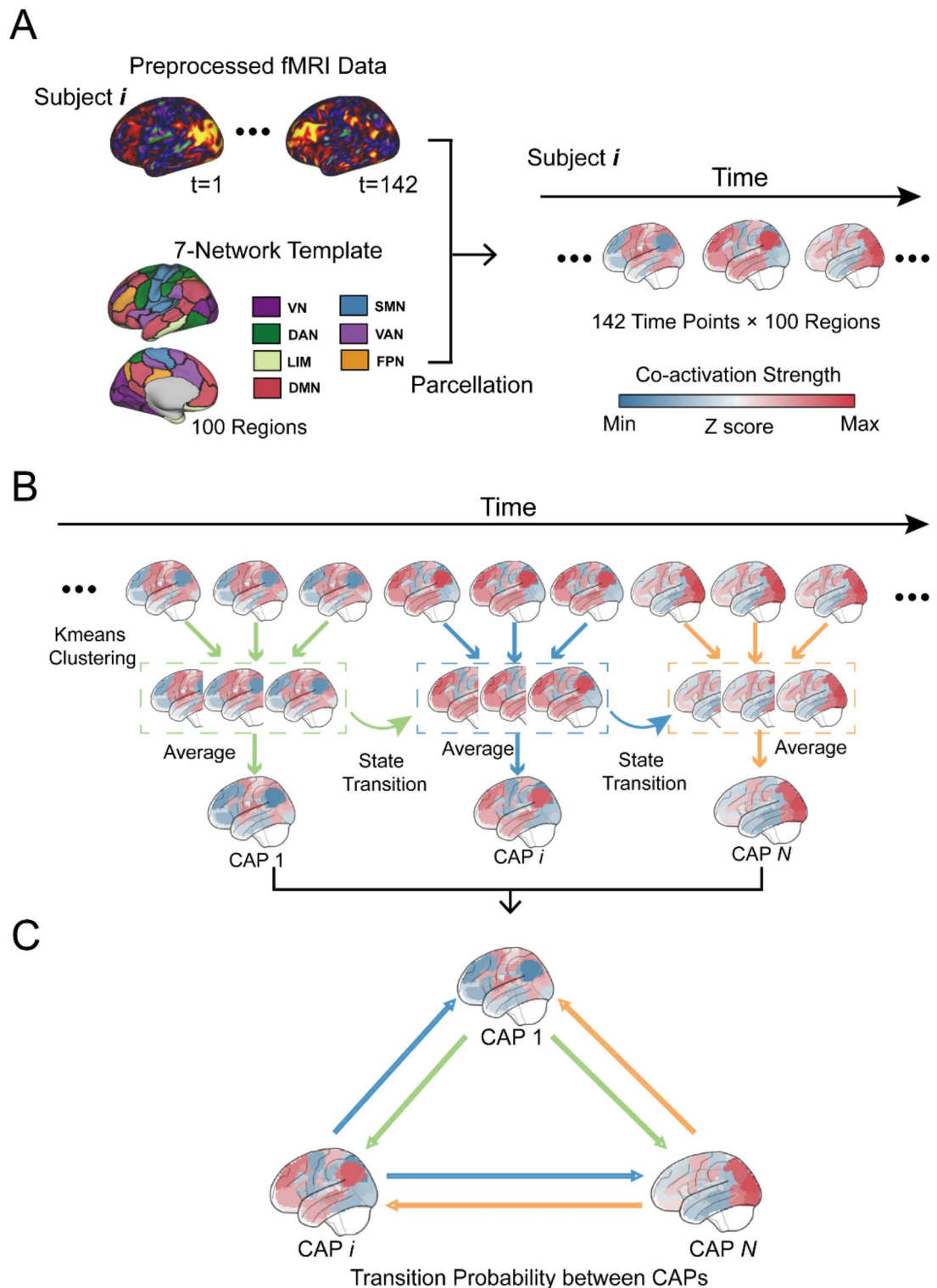


Fig. 1. The methodological overview of co-activation patterns (CAP) analysis. **(A)** The functional activity of each brain region was extracted using 7-network template. This resulted in a 142×100 brain activity matrix for each subject, where 142 represents the number of fMRI time points, and 100 corresponds to the number of brain regions. The color bar illustrates degree of strength of region-wise activation level, with red indicating the degree of activation and blue indicating the degree of deactivation for each brain region. **(B)** CAP states were identified using k-means clustering, which detects recurring states across time points with similar whole-brain co-activation patterns. The clustering process yielded N distinct clusters, where each cluster corresponds to a recurring CAP state. The spatial distribution of each CAP (such as CAP1, CAP i , ...CAP N) was defined by the average co-activation pattern of its corresponding cluster center. **(C)** For each subject, the state transition probabilities were calculated. The transition probability matrix represents the probability of transitioning from one state (CAP i) to another state (CAP j) at consecutive time points.

region of CAPs to the one of intrinsic functional network (ICNs). Our results indicated that CAP 1 was mainly related with the activated DAN, VAN; CAP 2 was mainly related with the activated SMN; CAP 3 was mainly related with the activated DMN, DAN; CAP 4 was mainly related with the activated DMN, LIM; CAP 5 was mainly related with the activated SMN, VN; CAP 6 was mainly related with the activated DAN, VAN; CAP 7 was mainly related with the activated DMN; CAP 8 was mainly related with the activated VN, DAN; CAP 9 was mainly related with the activated VAN; CAP 10 was mainly related with the activated FPN, DMN.

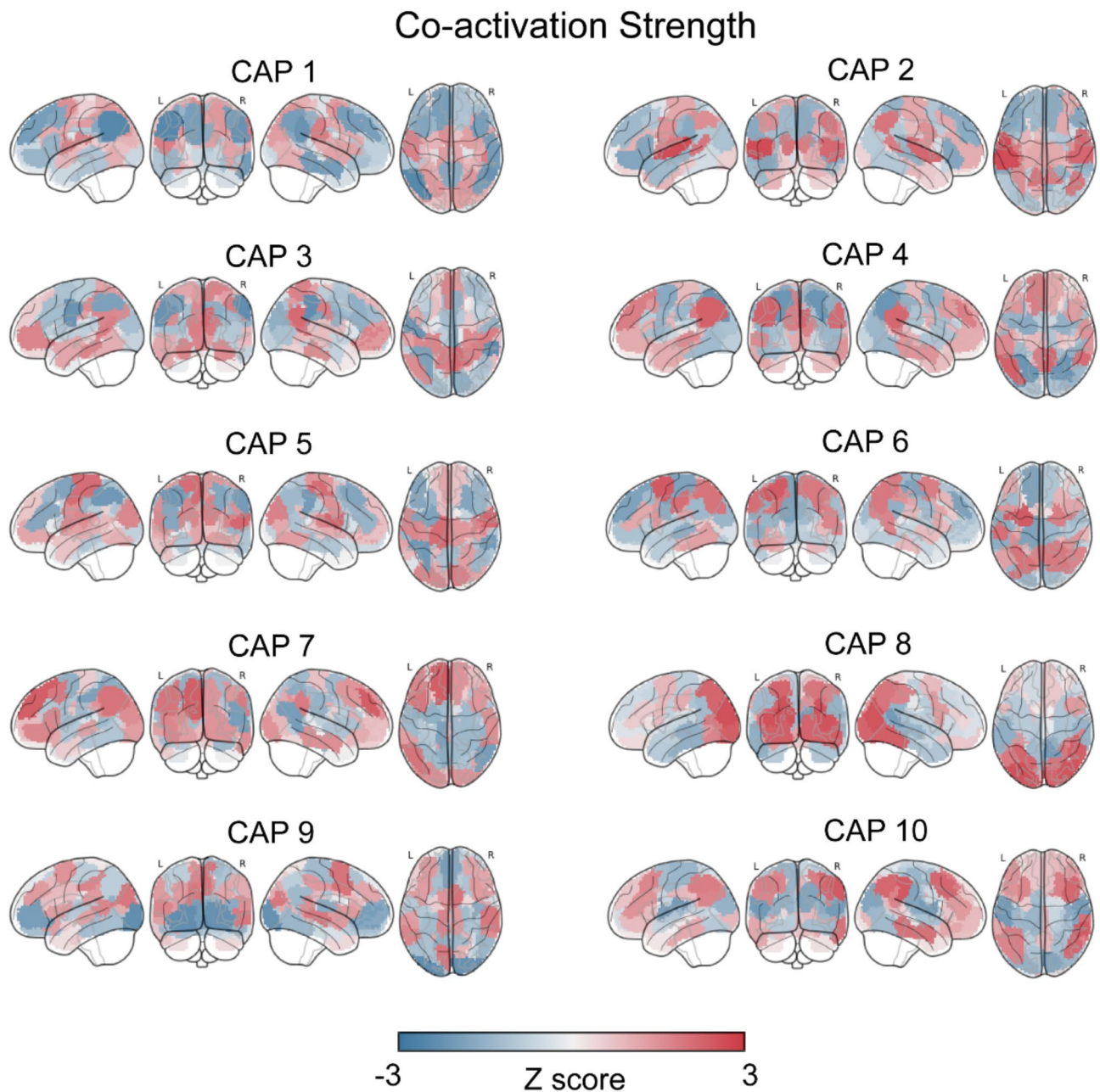


Fig. 2. The spatial distribution of each co-activation pattern (CAP). Each CAP map was normalized by z-score transformation to illustrate patterns of activation or deactivation (degree of strength to which the region-wise activation level deviate from zero). Our results indicated that CAP 1 was mainly related with the activated DAN, VAN; CAP 2 was mainly related with the activated SMN; CAP 3 was mainly related with the activated DMN, DAN; CAP 4 was mainly related with the activated DMN, LIM; CAP 5 was mainly related with the activated SMN, VN; CAP 6 was mainly related with the activated DAN, VAN; CAP 7 was mainly related with the activated DMN; CAP 8 was mainly related with the activated VN, DAN; CAP 9 was mainly related with the activated VAN; CAP 10 was mainly related with the activated FPN, DMN.

Abnormal state transition across SZ, BD, ADHD

We calculated fractional occupancy and transition probability for evaluating the aberrant dynamic properties within and between CAP states across different psychiatric disorders. Significant differences in state transitions were observed between psychiatric disorders, while the fractional occupancy within each state did not exhibit significant differences.

By conducting ANOVA analysis, our results revealed the abnormal state transitions across SZ, BD, ADHD. As showed in Fig. 3A and B, our results indicated that (1) there was a group difference in the transition probability from CAP 1 to CAP 4 between four groups ($F=3.11$, $P=0.027$, one-way ANOVA). Post-hoc analysis indicated that this transition probability is significantly reduced in individuals with BD compared to HC ($T=-2.52$, $P_{FDR}=0.038$, student t-test) and SZ ($T=-2.81$, $P_{FDR}=0.036$). (2) there was a group difference in the transition probability from CAP 1 to CAP 9 between four groups ($F=4.40$, $P=0.005$). Post-hoc analysis indicated that this transition probability is significantly increased in individuals with BD ($T=3.29$, $P_{FDR}=0.007$), SZ ($T=2.43$, $P_{FDR}=0.049$) compared to HC. (3) there was a group difference in the transition probability from CAP 1 to CAP 10 between four groups ($F=3.90$, $P=0.001$). Post-hoc analysis indicated that this transition probability is significantly increased in individuals with ADHD compared to HC ($T=3.31$, $P_{FDR}=0.007$). (4) there was a group difference in the transition probability from CAP 2 to CAP 3 between four groups ($F=4.05$, $P=0.008$). Post-hoc analysis indicated that this transition probability is significantly increased in individuals with BD compared to ADHD ($T=2.57$, $P_{FDR}=0.036$, student t-test) and SZ ($T=2.80$, $P_{FDR}=0.036$). (5) there was a group difference in the transition probability from CAP 2 to CAP 5 between four groups ($F=3.50$, $P=0.016$). Post-hoc analysis indicated that this transition probability is significantly increased in individuals with ADHD compared to BD ($T=2.79$, $P_{FDR}=0.040$). (6) there was a group difference in the transition probability from CAP 5 to CAP 8 between four groups ($F=4.07$, $P=0.007$). Post-hoc analysis indicated that this transition probability is significantly increased in individuals with BD compared to SZ ($T=2.79$, $P_{FDR}=0.040$), ADHD ($T=2.92$, $P_{FDR}=0.022$), and HC ($T=2.71$, $P_{FDR}=0.022$). (7) there was a group difference in the transition probability from CAP 7 to CAP 1 between four groups ($F=5.14$, $P=0.002$). Post-hoc analysis indicated that this transition probability is significantly increased in individuals with SZ compared to ADHD ($T=3.49$, $P_{FDR}=0.003$), and HC ($T=3.32$, $P_{FDR}=0.003$). (8) there was a group difference in the transition probability from CAP 9 to CAP 2 between four groups ($F=3.55$, $P=0.015$). Post-hoc analysis indicated that this transition probability is significantly reduced in individuals with BD compared to ADHD ($T=-2.58$, $P_{FDR}=0.035$), and HC ($T=-2.66$, $P_{FDR}=0.035$). (9) there was a group difference in the transition probability from CAP 10 to CAP 6 between four groups ($F=3.19$, $P=0.024$). Post-hoc analysis indicated that this transition probability is significantly reduced in individuals with BD compared to SZ ($T=-3.20$, $P_{FDR}=0.018$).

Analysis of core CAPs

Among the abnormal state transitions, CAP 1 and CAP 2 emerged as core states due to their higher out-degree and in-degree centrality. As showed in Fig. 3A, the results indicate that CAP 1 and CAP 2 exhibit significantly higher degree centrality values (both ≥ 3), while all other CAPs have degree centrality values ≤ 2 . Therefore, we investigated the spatial patterns, cognitive functions, and behavioral associations of the core states. Firstly, as showed in Fig. 4A, we found that the spatial pattern of CAP 1 was significantly associated to functional gradient ($R = -0.8$, $P < 0.001$). Then, we averaged the activity of each ICN in CAP 1. As showed in Fig. 4B, our results indicated that CAP 1 was mainly related with the activated attention network (DAN, VAN), SMN and deactivated high-level networks including DMN, and FPN. Next, to quantify the cognitive relevance of CAP 1, we utilized association mapping between the spatial pattern of CAP 1 and Neurosynth topics. As showed in Fig. 4C, CAP 1 has an association with visual, premotor, pain, somatosensory, and imagery functions. Last, to link the core CAPs and cognitive behavior, we calculated the Pearson correlation between state transition probability and behavioral measures. As showed in Fig. 4D, significantly correlations were detected between the transition probability from CAP 1 to CAP 10 and behavioral measures, including Wechsler Memory Scale (WMS, Visual reproduction delayed recall score, $R = -0.17$, $P=0.008$), and Wechsler Adult Intelligence Scale (WAIS-IV, Vocabulary score, $R = -0.18$, $P=0.005$; and Matrix reasoning score, $R = -0.18$, $P=0.005$).

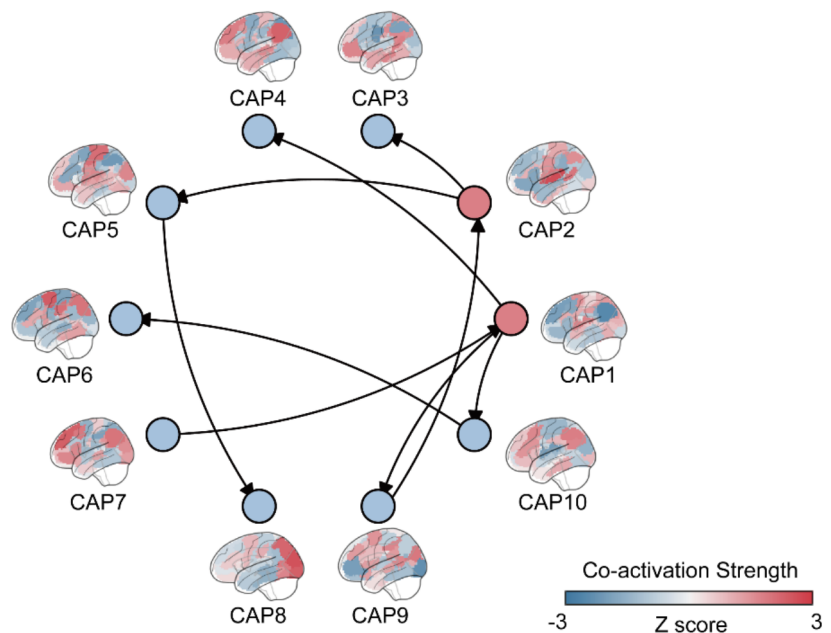
Discussion

In this study, we investigated the dynamic abnormalities among schizophrenia (SZ), bipolar disorder (BD), and attention-deficit/hyperactivity disorder (ADHD). By conducting CAP analysis, we identified abnormal transition patterns involving these three psychiatric disorders and found that different disorders exhibit distinct transition characteristics. Notably, these abnormal transitions were concentrated in core states (CAP 1 and CAP 2), whose spatial patterns were significantly associated with functional gradients. These findings suggest that the observed dynamic abnormalities are not random but are instead focused on transitions between specific states.

The abnormal state transitions identified in our study revealed significant specificity across the different psychiatric disease. For SZ, the transition probabilities from CAP 7 to CAP 1 and from CAP 1 to CAP 4 was significantly higher in individuals with SZ compared to other psychiatric diseases and HC. For BD, the transition probabilities from CAP2 to CAP3 and from CAP5 to CAP8 were significantly higher than those in HC and other psychiatric disorders. For ADHD, the transition probabilities from CAP1 to CAP10 and from CAP2 to CAP5 were significantly higher than those in HC and other disorders. Our results revealed the differences in state transitions among SZ, BD, and ADHD, and these disorder-specific dynamic transitions emphasize the distinct neural mechanisms underlying each psychiatric condition.

Despite these differences, the abnormalities across SZ, BD, and ADHD converged on core states (CAP 1 and CAP 2). CAP 1 primarily involved the attention networks (VAN, DAN) and the sensorimotor network (SMN), while CAP 2 reflected SMN activation. The predominance of these core states underscores a fundamental

A



B

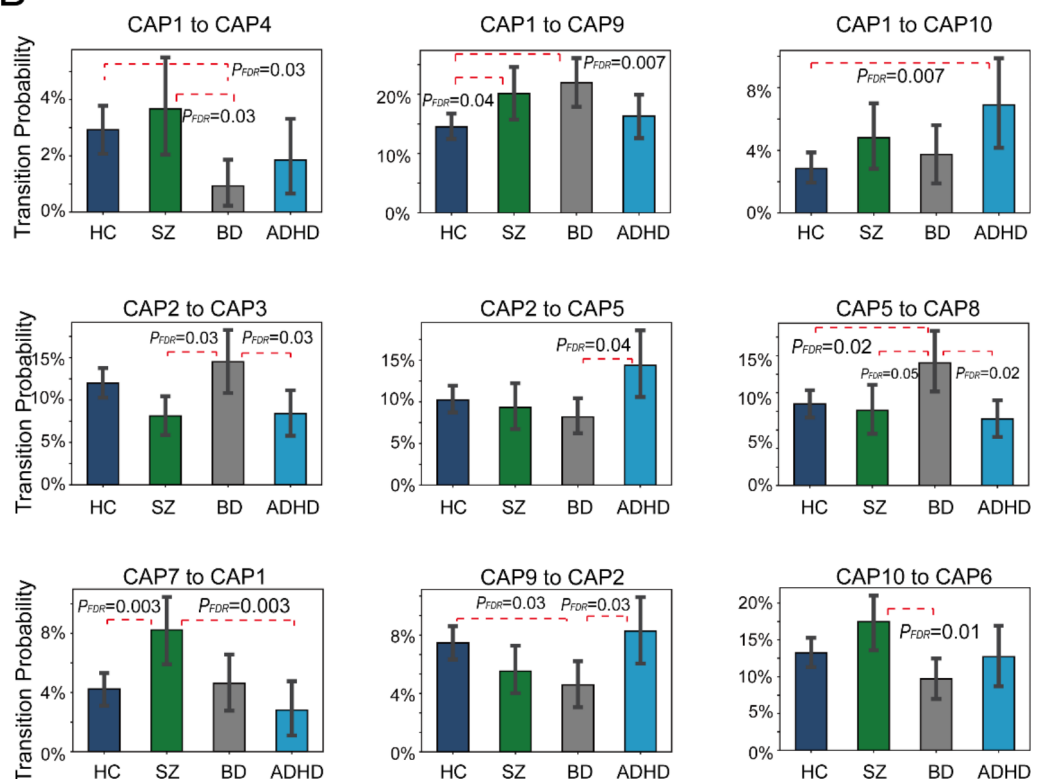


Fig. 3. (A) The abnormal state transitions were identified by conducting one-way ANOVA analysis across SZ, BD, ADHD, and HC. Specifically, CAP 1 and CAP 2 were identified as the core states, characterized by higher out-degree and in-degree centrality. (B) Post-hoc analysis (t test between each pair of conditions) revealed significant specificity across the different psychiatric disease.

commonality in the dynamic characteristics of these disorders, emphasizing the shared neural dysfunctions across psychiatric conditions. This focus on core states aligns with the brain's hierarchical functional organization, constrained by the functional gradient—a macroscale principle spanning from unimodal networks (primary sensory perceptual networks, such as SMN, VN) to transmodal networks (high-level cognitive networks, such as

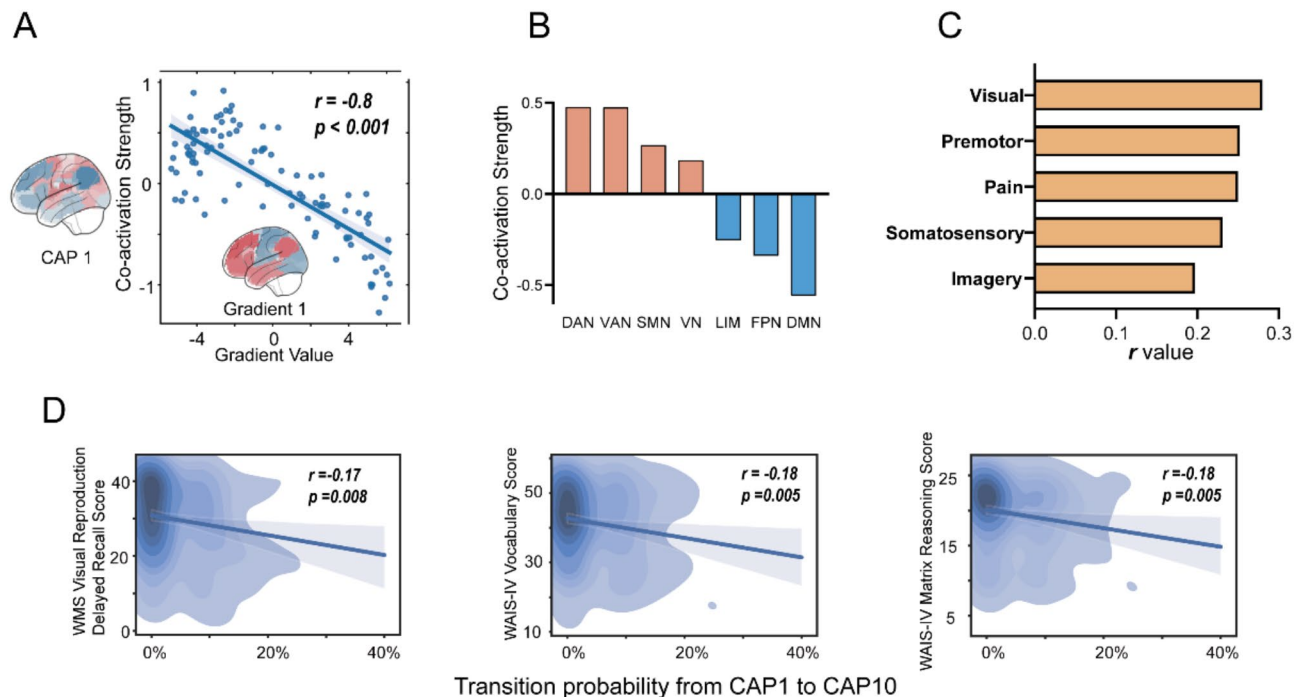


Fig. 4. (A) The spatial distribution of CAP 1 was significantly associated with the functional gradient ($R = -0.8$, $P < 0.001$) which captures the hierarchical organization of brain function, ranging from primary sensory-motor networks to high-level cognitive networks. (B) Using activation strength within intrinsic functional networks to characterize the spatial distribution of CAP 1, it was found to be mainly related to activated attention networks (DAN, VAN), the SMN, and deactivated high-level networks (DMN, FPN). (C) To quantify the functional relevance of CAP 1, association mapping between its spatial distribution and Neurosynth topics was conducted. The bar chart illustrates the most correlated Neurosynth topics (top 5), highlighting CAP 1's relevance to Visual, Premotor, Pain, Somatosensory, and Imagery functions. (D) Significant correlations were detected between the transition probability from CAP 1 to CAP 10 and behavioral measures, including Wechsler Memory Scale (WMS, Visual reproduction delayed recall score, $R = -0.17$, $P = 0.008$), and Wechsler Adult Intelligence Scale (WAIS-IV, Vocabulary score, $R = -0.18$, $P = 0.005$; and Matrix reasoning score, $R = -0.18$, $P = 0.005$).

DMN, FPN)²⁸. Previous studies have indicated that intrinsic brain activity exhibits spatiotemporal propagation patterns along functional gradient, with activation and deactivation systematically propagating between unimodal and transmodal networks^{29,30}. In our results, the core states (CAP 1 and CAP 2) were characterized by activation in unimodal networks. In contrast, other states, including CAP 3, CAP 4, CAP 7, and CAP 10, exhibit the opposite pattern—activation in transmodal networks and deactivation in unimodal networks. The significantly altered transition probabilities involving core states (e.g., from CAP7 to CAP1 and CAP1 to CAP4) may indicate atypical patterns of state switching between unimodal and transmodal network activations. These transitions reflect abnormalities in the brain's ability to dynamically coordinate activity between sensory-motor or attention networks and higher-order cognitive networks. Such abnormalities may underlie the impaired information processing and integration observed in psychiatric conditions, providing insights into their physiological and clinical relevance.

To further understand the shared dysfunctions across psychiatric conditions, it is essential to delve into the intrinsic functional networks underlying these core states and their functional significance.

The core states identified in our study prominently feature the activation of attention network and SMN. The attention networks, including VAN and DAN, are critical for directing and sustaining attention. VAN is involved in detecting and responding to salient stimuli, and its dysfunction can lead to difficulties in processing and responding to important environmental cues³¹. DAN is responsible for top-down, goal-directed attention, enabling sustained focus on relevant tasks and suppressing distractions. Abnormalities in this network can result in impaired executive function and attention regulation³². Dysfunctions in attention networks are implicated in psychiatric disorders. In SZ, patients often exhibit impaired attention network function, leading to difficulties in sustaining attention and increased distractibility³³. Moreover, aberrant morphology and functional connectivity in the VAN has been reported, contributing to the cognitive deficits observed in SZ¹⁰. By summarizing the emerged evidence of structural and functional brain studies, Menon et al. found the aberrant dynamic temporal interactions in triple network, including FPN, DMN and salience network (VAN), and highlight the central role of the VAN in the aberrant mapping of salient external and internal events in SZ³⁴. In BD, patients also demonstrate disruptions in attention networks, particularly during manic and depressive episodes, which affect their ability to focus and process information³⁵. Neuroimaging evidence indicated that the connectivity

between DAN and FPN are significantly altered at task-based situations³⁶, and the significantly reduced functional connectivity between VAN and FPN was found³⁷. ADHD is characterized by deficits in attention and cognitive control³⁸, and the abnormal attention networks are believed to contribute to the core symptoms of inattention and hyperactivity in ADHD. Resting-state fMRI studies provided evidence that the abnormal interconnections between VAN and DMN are the key locus of dysfunction in ADHD³⁹. Moreover, Cai et al. identified abnormalities in task-induced modulation of connectivity within the VAN and the FPN in children with ADHD, highlighting that cingulo-frontal connectivity represented a common locus of impairment in cognitive control and clinical assessments of inattention symptoms⁴⁰. Our results identified aberrant in state transitions characterized by attention networks, and highlighting the shared abnormality across different psychiatric disorders.

We also found that the core state involves activation of the SMN. Sensory and motor dysfunction have been reported in SZ⁴¹, BD⁴², and ADHD⁴³. Specifically, Kebets et al. conducted transdiagnostic approach to identify latent components linking the large-scale functional networks to the behavior measures. This study indicated that SMN is the transdiagnostic hubs, and showed that dysconnectivity patterns of SMN are linked to variation in three domains: general psychopathology, cognitive dysfunction across SZ, BD, ADHD¹¹. These above findings are based on static functional network analysis. Our results further emphasize the importance of the SMN across psychiatric disorders from a dynamic perspective.

Limitations

A key limitation of this study is the low temporal resolution of fMRI, which may hinder the capture of rapid neural dynamics underlying brain activity, potentially leading to an incomplete characterization of abnormal neural dynamics in psychiatric disorders. Future studies could integrate fMRI with modalities such as MEG or EEG, which offer higher temporal resolution, enabling a more comprehensive investigation of neural dynamics. Additionally, schizophrenia (SZ) group in our study has a disproportionately higher number of male participants. This gender imbalance is inherent in the publicly available dataset used in our analysis. While this may limit the generalizability of the findings to female populations, it is important to emphasize that the value of this dataset lies in its large-scale, single-site, and cross-disease design, providing valuable insights into shared and specific neural characteristic across different psychiatric conditions.

Conclusion

This study investigated the dynamic configurations of brain activity across SZ, BD, and ADHD based on the CAP method. We found that while these disorders exhibit distinct state transition patterns, their abnormalities converge on core states involving the attention and sensorimotor networks, significantly correlating with the functional gradient. By highlighting shared and specific dynamic abnormalities, our research advances the understanding of the neurobiological mechanisms underlying psychiatric conditions.

Data availability

The datasets (UCLA CNP data) analysed during the current study are available in the public database OpenfMRI (<https://openneuro.org/datasets/ds000030/versions/00016>).

Received: 13 October 2024; Accepted: 24 January 2025

Published online: 01 April 2025

References

1. Sha, Z. Q., Wager, T. D., Mechelli, A. & He, Y. Common dysfunction of large-scale Neurocognitive Networks Across Psychiatric disorders. *Biol. Psychiatry*. **85**, 379–388. <https://doi.org/10.1016/j.biopsych.2018.11.011> (2019).
2. Xia, C. H. et al. Linked dimensions of psychopathology and connectivity in functional brain networks. *Nat. Commun.* **9** <https://doi.org/10.1038/s41467-018-05317-y> (2018).
3. Smoller, J. W. & Cross Disorder Group of the Psychiatric Genomics Consortium. vol 381, pg 1371., Identification of risk loci with shared effects on five major psychiatric disorders: a genome-wide analysis *Lancet* **381**, 1360–1360 (2013). (2013).
4. Caspi, A. et al. The p factor: one General psychopathology factor in the structure of Psychiatric disorders? *Clin. Psychol. Science: J. Association Psychol. Sci.* **2**, 119–137 (2014).
5. Kendler, K. S. et al. The structure of genetic and environmental risk factors for <i>DSM-IV</i> Personality disorders a Multivariate Twin Study. *Arch. Gen. Psychiatry*. **65**, 1438–1446. <https://doi.org/10.1001/archpsyc.65.12.1438> (2008).
6. Sprooten, E. et al. Addressing reverse inference in Psychiatric Neuroimaging: Meta-analyses of Task-related brain activation in Common Mental disorders. *Hum. Brain. Mapp.* **38**, 1846–1864. <https://doi.org/10.1002/hbm.23486> (2017).
7. Baker, J. T. et al. Disruption of Cortical Association Networks in Schizophrenia and psychotic bipolar disorder. *Jama Psychiatry*. **71**, 109–118. <https://doi.org/10.1001/jamapsychiatry.2013.3469> (2014).
8. Goodkind, M. et al. Identification of a common neurobiological substrate for Mental Illness. *Jama Psychiatry*. **72**, 305–315. <https://doi.org/10.1001/jamapsychiatry.2014.2206> (2015).
9. Buckner, R. L., Andrews-Hanna, J. R. & Schacter, D. L. in *Year in Cognitive Neuroscience 2008* Vol. 1124 *Annals of the New York Academy of Sciences* (eds A. Kingstone & M. B. Miller) 1–38 (2008).
10. Menon, V. Large-scale brain networks and psychopathology: a unifying triple network model. *Trends Cogn. Sci.* **15**, 483–506. <https://doi.org/10.1016/j.tics.2011.08.003> (2011).
11. Kebets, V. et al. Somatosensory-motor dysconnectivity spans multiple transdiagnostic dimensions of psychopathology. *Biol. Psychiatry*. **86**, 779–791. <https://doi.org/10.1016/j.biopsych.2019.06.013> (2019).
12. Uddin, L. Q. Cognitive and behavioural flexibility: neural mechanisms and clinical considerations. *Nat. Rev. Neurosci.* **22**, 167–179. <https://doi.org/10.1038/s41583-021-00428-w> (2021).
13. Xiao, J. M. et al. A spatio-temporal decomposition framework for dynamic functional connectivity in the human brain. *Neuroimage* **263** <https://doi.org/10.1016/j.neuroimage.2022.119618> (2022).
14. Li, C. et al. Transdiagnostic time-varying dysconnectivity across major psychiatric disorders. *Hum. Brain. Mapp.* **42**, 1182–1196. <https://doi.org/10.1002/hbm.25285> (2021).

15. Liu, X. & Duyn, J. H. Time-varying functional network information extracted from brief instances of spontaneous brain activity. *Proc. Natl. Acad. Sci. U.S.A.* **110**, 4392–4397. <https://doi.org/10.1073/pnas.1216856110> (2013).
16. Janes, A. C., Peechatka, A. L., Frederick, B. B. & Kaiser, R. H. Dynamic functioning of transient resting-state coactivation networks in the human Connectome Project. *Hum. Brain. Mapp.* **41**, 373–387. <https://doi.org/10.1002/hbm.24808> (2020).
17. Kaiser, R. H. et al. Abnormal fronto-insular-default network dynamics in adolescent depression and rumination: a preliminary resting-state co-activation pattern analysis. *Neuropsychopharmacology* **44**, 1604–1612. <https://doi.org/10.1038/s41386-019-0399-3> (2019).
18. Ma, X. Y. et al. Altered temporal Organization of brief spontaneous brain activities in patients with Alzheimer's Disease. *Neuroscience* **425**, 1–11. <https://doi.org/10.1016/j.neuroscience.2019.11.025> (2020).
19. Li, L., Zheng, Q. Y., Xue, Y., Bai, M. S. & Mu, Y. M. Coactivation pattern analysis reveals altered whole-brain functional transient dynamics in autism spectrum disorder. *Eur. Child Adolesc. Psychiatry*. <https://doi.org/10.1007/s00787-024-02474-y> (2024).
20. Yang, H. et al. Reproducible coactivation patterns of functional brain networks reveal the aberrant dynamic state transition in schizophrenia. *Neuroimage* **237** <https://doi.org/10.1016/j.neuroimage.2021.118193> (2021).
21. Poldrack, R. A. et al. A phenome-wide examination of neural and cognitive function. *Sci. Data*. **3** <https://doi.org/10.1038/sdata.2016.110> (2016).
22. Esteban, O. et al. fMRIPrep: a robust preprocessing pipeline for functional MRI. *Nat. Methods*. **16**, 111–. <https://doi.org/10.1038/s41592-018-0235-4> (2019).
23. Smith, S. M. et al. Resting-state fMRI in the human Connectome Project. *Neuroimage* **80**, 144–168. <https://doi.org/10.1016/j.neuroimage.2013.05.039> (2013).
24. Yan, L. R. et al. Physiological origin of low-frequency drift in blood oxygen level dependent (BOLD) functional magnetic resonance imaging (fMRI). *Magn. Reson. Med.* **61**, 819–827. <https://doi.org/10.1002/mrm.21902> (2009).
25. Gratton, C. et al. Removal of high frequency contamination from motion estimates in single-band fMRI saves data without biasing functional connectivity. *Neuroimage* **217** <https://doi.org/10.1016/j.neuroimage.2020.116866> (2020).
26. Triana, A. M., Glerean, E., Saramäki, J. & Korhonen, O. Effects of spatial smoothing on group-level differences in functional brain networks. *Netw. Neurosci.* **4**, 556–574. https://doi.org/10.1162/netn_a_00132 (2020).
27. Schaefer, A. et al. Local-Global Parcellation of the Human Cerebral Cortex from Intrinsic Functional Connectivity MRI. *Cerebral cortex (New York, N.Y.: 28, 3095–3114, (1991).* <https://doi.org/10.1093/cercor/bhx179> (2018).
28. Margulies, D. S. et al. Situating the default-mode network along a principal gradient of macroscale cortical organization. *Proc. Natl. Acad. Sci. U.S.A.* **113**, 12574–12579. <https://doi.org/10.1073/pnas.1608282113> (2016).
29. Yousefi, B. & Keilholz, S. Propagating patterns of intrinsic activity along macroscale gradients coordinate functional connections across the whole brain. *Neuroimage* **231** <https://doi.org/10.1016/j.neuroimage.2021.117827> (2021).
30. Park, B. Y. et al. Signal diffusion along connectome gradients and inter-hub routing differentially contribute to dynamic human brain function. *Neuroimage* **224** <https://doi.org/10.1016/j.neuroimage.2020.117429> (2021).
31. Corbetta, M. & Shulman, G. L. Control of goal-directed and stimulus-driven attention in the brain. *Nat. Rev. Neurosci.* **3**, 201–215. <https://doi.org/10.1038/nrn755> (2002).
32. Vossel, S., Geng, J. J. & Fink, G. R. Dorsal and ventral attention systems: distinct neural circuits but collaborative roles. *Neuroscientist* **20**, 150–159. <https://doi.org/10.1177/1073858413494269> (2014).
33. Barch, D. M. & Ceaser, A. Cognition in schizophrenia: core psychological and neural mechanisms. *Trends Cogn. Sci.* **16**, 27–34. <https://doi.org/10.1016/j.tics.2011.11.015> (2012).
34. Menon, V., Palaniyappan, L. & Supekar, K. Integrative Brain Network and Salience models of psychopathology and cognitive dysfunction in Schizophrenia. *Biol. Psychiatry*. **94**, 108–120. <https://doi.org/10.1016/j.biopsych.2022.09.029> (2023).
35. Pomarol-Clotet, E. et al. Brain functional changes across the different phases of bipolar disorder. *Br. J. Psychiatry*. **206**, 136–144. <https://doi.org/10.1192/bjp.bp.114.152033> (2015).
36. Das, P., Calhoun, V. & Malhi, G. S. Bipolar and borderline patients display differential patterns of functional connectivity among resting state networks. *Neuroimage* **98**, 73–81. <https://doi.org/10.1016/j.neuroimage.2014.04.062> (2014).
37. Wang, J. J. et al. Shared and specific functional connectivity alterations in unmedicated bipolar and major depressive disorders based on the triple-network model. *Brain Imaging Behav.* **14**, 186–199. <https://doi.org/10.1007/s11682-018-9978-x> (2020).
38. Castellanos, F. X. & Tannock, R. Neuroscience of attention-deficit/hyperactivity disorder: the search for endophenotypes. *Nat. Rev. Neurosci.* **3**, 617–628. <https://doi.org/10.1038/nrn896> (2002).
39. Sripada, C. et al. Disrupted Network Architecture of the resting brain in Attention-Deficit/Hyperactivity disorder. *Hum. Brain. Mapp.* **35**, 4693–4705. <https://doi.org/10.1002/hbm.22504> (2014).
40. Cai, W. D., Griffiths, K., Korgaonkar, M. S., Williams, L. M. & Menon, V. Inhibition-related modulation of salience and frontoparietal networks predicts cognitive control ability and inattention symptoms in children with ADHD. *Mol. Psychiatry*. **26**, 4016–4025. <https://doi.org/10.1038/s41380-019-0564-4> (2021).
41. Javitt, D. C. & Freedman, R. Sensory Processing Dysfunction in the personal experience and neuronal Machinery of Schizophrenia. *Am. J. Psychiatry*. **172**, 17–31. <https://doi.org/10.1176/appi.ajp.2014.13121691> (2015).
42. Giakouraki, S. G. et al. Evidence of disrupted prepulse inhibition in unaffected siblings of bipolar disorder patients. *Biol. Psychiatry*. **62**, 1418–1422. <https://doi.org/10.1016/j.biopsych.2006.12.002> (2007).
43. Shimizu, V. T., Bueno, O. F. A. & Miranda, M. C. Sensory processing abilities of children with ADHD. *Braz. J. Phys. Ther.* **18**, 343–352. <https://doi.org/10.1590/bjpt-rbf.2014.0043> (2014).

Author contributions

Conception and design were conducted by Lianjie NIU, Jinrong Qu and Xianfu Sun; administrative support was conducted by Xianfu Sun; the provision of study materials or patients was completed by Keke Fang and Shaoqiang Han; the collection and assembly of data was conducted by Lianjie Niu, Wenshi Li and Peng Liu; data analysis and interpretation were conducted by Lianjie Niu, Wenshi Li, Keke Fang, Shaoqiang Han, Peng Liu; manuscript writing was conducted by all authors. All authors read and approved the final version of the manuscript.

Funding

The present study was supported by the Department of Science and Technology of Henan Province focuses on R&D and promotion of special scientific and technological research projects (grant no. 212102310138 and 222102310512) and the Natural Science Foundation of Henan Province Youth Project (grant no. 242300420414).

Declarations

Competing interests

The authors declare no competing interests.

Additional information

Correspondence and requests for materials should be addressed to J.Q. or X.S.

Reprints and permissions information is available at www.nature.com/reprints.

Publisher's note Springer Nature remains neutral with regard to jurisdictional claims in published maps and institutional affiliations.

Open Access This article is licensed under a Creative Commons Attribution-NonCommercial-NoDerivatives 4.0 International License, which permits any non-commercial use, sharing, distribution and reproduction in any medium or format, as long as you give appropriate credit to the original author(s) and the source, provide a link to the Creative Commons licence, and indicate if you modified the licensed material. You do not have permission under this licence to share adapted material derived from this article or parts of it. The images or other third party material in this article are included in the article's Creative Commons licence, unless indicated otherwise in a credit line to the material. If material is not included in the article's Creative Commons licence and your intended use is not permitted by statutory regulation or exceeds the permitted use, you will need to obtain permission directly from the copyright holder. To view a copy of this licence, visit <http://creativecommons.org/licenses/by-nc-nd/4.0/>.

© The Author(s) 2025